

P-V relationship of elements in the pressure range of 200–300 GPa

Yuichi Akahama and Masaaki Geshi

*Graduate school of Science, University of Hyogo, 3-2-1 Kamigohri, Hyogo 678-1297, Japan and
R³ Institute for Newly-Emerging Science Design, Osaka University,
1-2, Machikaneyama, Toyonaka, 560-0043, Japan*

(Dated: August 19, 2024)

In this study, we analyzed the pressure-volume (P - V) relationship of elements using the equation of state at an ambient temperature within the multi-megabar pressure range of 200–300 GPa. We investigated the compressibility of elements under ultra-high pressures based on their positions in the periodic table. For the elemental materials in this region, pressure (P) can be approximated as an N -order function of volume (V): $P \propto 1/V^N$. By determining the N value, we can evaluate the contribution of the volume change to the total energy of the system. The N value is also an indicator the bulk modulus in this pressure range and shows periodicity with increasing atomic number, and shows significant values in the range of 4.5–6, for transition metals with close-packed structures (fcc, hcp). This suggests that the total energy of these elements increases rapidly as volume decreases. Furthermore, the current results provide basic data for understanding the compressibility of elemental materials under extreme ultra high-pressure conditions based on the quantum theory of solids.

I. I. INTRODUCTION

In recent years, the development of ultrahigh-pressure synchrotron X-ray diffraction technique,[1, 2] combined with advancements in first-principles calculation methods, has led to the elucidation of structural phase transitions and equations of state (EOS) for nearly all elemental materials under ultrahigh pressures. Using these experimental techniques, we have clarified the structural phase transitions for approximately 30 types of elements under ultrahigh-pressure conditions as well as the EOS of each high-pressure phase.[3–9] These studies have revealed that nearly all elements exhibit metallic behavior in the multi-megabar pressure range, often accompanied by structural phase transitions.

Currently, EOSs for many elements at room temperature are proposed based on pressure-volume (P - V) data obtained from X-ray diffraction experiments in high-pressure regions. Pressure (P) is normally expressed as a function of volume: $P = F(V)$. This is commonly represented by the Birch–Murnaghan (BM)[10] equation and/or Vinet[11] equation of (1) and (2), as shown below:

$$P = (3/2)K_0(x^{7/3} - x^{5/3}) \cdot [1 + (3/4)(K'_0 - 4)(x^{2/3} - 1)], \quad (1)$$

and

$$P = 3K_0[(1 - x^{1/3})/x^{2/3}] \cdot \exp [3/2(K'_0 - 1)(1 - x^{1/3})], \quad (2)$$

where $x = V/V_0$ and K_0 and K'_0 correspond to the bulk modulus at normal pressure and the pressure derivative of K_0 , respectively. However, because both equations express pressure as a complicated function of volume, understanding the compression properties of these elements in the extreme high-pressure region is challenging.

In this study, we provide an overview of the ultrahigh-pressure world of materials by examining the atomic volumes and P - V relationships of elements in the range of 200–300 GPa based on the periodic table. Our findings show that in this ultrahigh-pressure range, pressure can be approximated as a simple function of volume: $P \propto 1/V^N$ with a parameter N . For transition metals, N has significant values in the range of 4.5–6, indicating that pressure has a strong dependence on volume. The obtained results provide important information for the advancement of not only high-pressure science but also materials science as well as earth and planetary science.

II. II. ANALYSIS

The atomic volumes (V_{200} and V_{300}) at 200 and 300 GPa for each element at an ambient temperature and the ratio of $V_{300}/V_{0\text{amb}}$, where $V_{0\text{amb}}$ corresponds to the atomic volume of the stable phase under ambient conditions, were estimated based on the EOS obtained from the X-ray diffraction experiments. The $\log(P)$ - $\log(V)$ plot for each element showed good linearity in the pressure range of 200 to 300 GPa. Therefore, we performed a linear approximation ($\log(P) \propto -N \log(V)$) in this region to estimate the coefficient N . Fig. 1 shows the $\log(P) - \log(V)$ plots for Ni,[9] Pt,[12–14] and Bi.[15] From these figures it is found that $\log(P)$ and $\log(V)$ exhibit relatively good

linearity in the multi-megabar pressure range of 200–300 GPa. The standard deviation of the N values was within 0.5%. In this pressure range, a simple relational expression between P and V holds true,

$$P \propto 1/V^N. \quad (3)$$

In this study, we also incorporated data from other studies. In cases where the maximum pressure (P_{\max}) in measurements did not reach 300 GPa, the reported EOSs were extrapolated. Some of these cases had P_{\max} value of less than 100 GPa. The pressure scale used was the Pt–EOS developed by Holmes *et al.*, [12] and the obtained N value was approximated 1% smaller than that of the Pt–EOS recently revised by Fratanduono *et al.* [14] By contrast, for the Pt–EOS proposed by Dewaele *et al.*, [13] the N value was 5.5% smaller. Furthermore, the Ag [16] data were recalculated using the Au scale developed by Fratanduono *et al.* [14] In addition, although the EOS proposed by other researchers were often used pressure scales different from the Pt–EOS proposed by Holmes *et al.*, [12] these EOSs were used in the analysis without pressure scale correction. The P – V curves Pt–EOSs reported by Holmes *et al.*, Dewaele *et al.*, and Fratanduono *et al.* and pressure differences among them are shown in Fig. S1.

The EOS data for elements and the obtained results in this analysis are listed in Table I, including atomic No., element symbol, P_{\max} , atomic volume at ambient pressure (V_0), bulk modulus (K_0), pressure derivative of K_0 (K'_0), EOS formula: Vinet (V), Birch-Murnaghan (BM), and AP1 (polynomial, see Ref. 37), atomic volumes at 200 GPa and 300 GPa (V_{200} and V_{300}), atomic volume of the ambient pressure phase under ambient condition ($V_{0\text{amb}}$), volume ratio ($V_{300}/V_{0\text{amb}}$), crystal structure/phase, and reference number. The column of the structure/phase shows the high-pressure structure or phase of the EOS based on the references. Some of EOSs are estimated from P-V data of two phases (see the references for the structure notation and its details). Note that the EOSs for β -Po type-S and hcp-Sn were calculated assuming the atomic volumes at 132 and 157 GPa to be V_0 , respectively. The EOS of bcc-Hf was recalculated using Vinet's equation, assuming the atomic volume 15.32 Å³ at 60.9 GPa to be V_0 . The EOS of hcp-Be [17] was calculated using Vinet's formula.

III. III. RESULTS AND DISCUSSION

Fig. 2 shows the changes in the atomic volume at 200 and 300 GPa (V_{200} and V_{300}), the volume ratio $V_{300}/V_{0\text{amb}}$, and the coefficient N with respect to the atomic number. The solid and broken vertical lines correspond to the periods of the elements and boundaries between the transition elements and typical elements or alkaline earth metals, respectively. Elements with P_{\max} higher than around 200 GPa are indicated in blue. Note that by assuming $N = 4$ in this pressure region, the uncertainty in V_{200} and V_{300} is estimated to be 1.8%, even with a 10% pressure uncertainty due to differences in pressure scales; this falls within the symbol. Estimating the error in the atomic volumes V_{200} and V_{300} obtained by (1) extrapolating the EOS estimated from P – V data with P_{\max} of 100 GPa or less to the multi-megabar region and (2) estimating from the EOS of elements that exhibit structural phase transitions in the multi-megabar pressure region is notably difficult. Therefore, these data should be considered reference values. In particular, regarding the BM equation with P_{\max} of 100 GPa or less and K'_0 of approximately three less, such as Be, Y, and Hf, we know that the P – V curve sometimes exhibits abnormal behavior when the equation is extrapolated up to 250 GPa. Therefore, extrapolated P – V curves for Be, Y, and Hf were examined. Consequently, unnatural behavior was observed for Hf (Fig. S2). The EOS of bcc-Hf was recalculated using the Vinet formula. In addition, to evaluate the difference in the pressure scale, the EOS of Ta obtained using the Pt–EOS scale proposed by Dewaele *et al.*, [13] was recalculated using the Pt–EOS scale proposed by Holmes *et al.* [12] The recalculated results for Hf, Ta, and Pt have been added to Table I and are shown in Fig. 2 with red symbols.

Under such ultrahigh pressures, the atomic volumes V_{200} and V_{300} exhibit considerably smaller values than those at normal pressure, [18] and the range of variation associated with changes in the atomic number is also small. In particular, the atomic volumes of the transition metals in periods 3–5 (PO. 3–5) are smaller than those of typical elements. Furthermore, the elements with the minimum atomic volume correspond to those near the center of transition metals in the periodic table, that is, those with d -electron numbers in the range of 6–8. The $V_{300}/V_{0\text{amb}}$ ratios of the transition metals in periods 3–5 are also large and incompressible compared to typical elements and exhibit a dome-shaped systematic atomic number dependence. Notably, even transition metals of Cu, Ag, and Au with relatively small K_0 and a close-packed structure are incompressible in this pressure range. On the other hand, the group 4–6 elements Ti, Zr, Hf, V, Nb, Ta, Cr, Mo, and W, having a bcc structure among transition metals, are relatively easily compressed and have a small volume ratio of $V_{300}/V_{0\text{amb}}$, and their N values are also smaller those with a close-packed structure. In addition, many elements exhibited N values approximated four, and elements with relatively small V_{200} and V_{300} tended to have large N values. High-pressure metallic phases of Mg, P, and S of PO. 2 behave as a simple metal with a bcc structure or a similar structure with pseudo-8 coordination, and their N values are small approximately 2.5.

As mentioned earlier, the P - V relationship of most elements can be approximated by formula (3) using the coefficient N in the range of 200–300 GPa. As shown in Table I, the standard deviation of N values was within 0.5%. Therefore, if the bulk modulus at pressure P is K_P , the following formula holds:

$$N = -d \log(P)/d \log(V) = -(V/P) \cdot (dP/dV) = K_P/P \quad (4)$$

Thus, K_P in this region can be estimated from the following equation:

$$K_P = N \cdot P \quad (5)$$

The parameter N is also an indicator of the bulk modulus in this pressure range. If K_P is first approximated as $K_P = K_0 + K'_0 \cdot P$ (K_0, K'_0 are constant), the following relationship holds true:

$$K'_0 = dK_P/dP = N, \quad (6)$$

which implies, N corresponds to K'_0 . For transition metals, the K'_0 values obtained from the experiments and N values showed good correspondence, indicating that this relationship can be applied. Thus, the P - V relationship can be described simply in the multi-megabar region of 200–300 GPa. However, this discussion is limited to the pressure range 200–300 GPa and cannot be applied when a phase transition is involved in this pressure range.

The P - V relations for the molecular solids H_2 , He, Ne, N_2 ,^[58] O_2 , Ar, Kr, and Xe are shown in Fig. 3. The volume values for H, N, and O correspond to H_2 , N_2 , and O_2 , respectively. The solidification pressure of each solid were indicated by arrows. Solid H_2 and He have N values of 2.27 and 2.46, respectively, and are more compressible than other molecules whereas solid Ne, N_2 ,^[58] O_2 , Ar, Kr, and Xe have similar N values in the range of 3.3–3.5. This may be because the wave functions of the $2s$ and $3s$ electrons occupying the outer orbitals of O_2 , N_2 , and Ne, Ar, Kr, and Xe molecules are required to be orthogonal to the wave function of the $1s$ electron, but the $1s$ electron cloud surrounding the H_2 and He molecules do not have this orthogonality constraint.^[59]

Elements with close-packed structures (fcc and hcp) exhibit relatively large N values. This is particularly noticeable for transition metals, where the N value reaches 4.5–6. This is because the d electrons localized around the nucleus are a source of large cohesive energy. Therefore, by further compressing a state in which the electron density is already high, the volume reduction seems to cause a rapid increase in the total electron kinetic energy.

Focusing on the individual elements, for Mn, a phase transition to the hcp structure is proposed at approximately 165 GPa; therefore, measuring the EOS of the hcp phase is necessary. Notably, the V_{200} and V_{300} values of Hf are smaller than those of other $3d$ transition metals.

We were interested in determining why transition metals have large N values of 4.5–6. In a solid, under ultrahigh pressure (200–300 GPa), the following quantum theoretical effects are expected to play a role: (1) the Pauli exclusion principle, (2) orthogonality constraints with core electrons, (3) relativistic effects for heavy elements, and (4) the correlation of d -electrons (although magnetism disappears under ultrahigh pressure). These quantum theoretical effects must be closely related to the total energy E_{in} . Understanding the physical features of an extremely high-density state of matter using quantum theory is important for comprehending the behavior of materials under ultrahigh-pressure conditions.

Finally, in the quantum theory of condensed materials, pressure is defined as the volumetric derivative of the total energy E_{in} (internal energy at temperature (T) = 0 K): $-P = dE_{in}/dV$. Namely, in this pressure range, E_{in} is expressed as an $N - 1$ order function of V : $E_{in} \propto 1/V^{(N-1)}$. E_{in} is the sum of the total kinetic energy of the electrons E_k , electrostatic interaction E_{es} , and exchange-correlation interaction, E_{xc} . We also analyzed the EOS of transition metals obtained from previously reported density functional theory calculations. The results obtained are in good agreement with the results of this analysis. However, because we have not yet examined the calculation methods and results in detail, we refrain from showing these analytical results and comparing them with the experimental results.

IV. IV. CONCLUSION

The current study demonstrated that for nearly all elements, P could be very well approximated as an N -order function of V in the multi-megabar pressure region between 200 and 300 GPa, allowing us to easily evaluate the contribution of the volume change to pressure, *i.e.*, the total energy of the system. We were able to discuss the compressibility of elements systematically. However, experimental data in this pressure range are still insufficient, and the current study also suggests the need for further experimental and theoretical research on elements in the pressure range. We hope that the results obtained in this analysis will serve as basic data for future ultrahigh-pressure research.

V. SUPPLEMENTARY MATERIAL

See the Supplementary Material for the comparison among equations of state of Pt proposed by previous studies and the P - V curve for the revised EOS of bcc-Hf using the Vinet equation.

VI. DATA AVAILABILITY

The data that support the findings of this study are available from the corresponding author upon reasonable request.

-
- [1] Y. Akahama, M. Nishimura, H. Kawamura, N. Hirao, Y. Ohishi, and K. Takemura, *Phys. Rev. B* **82**, 060101(R) (2010).
 - [2] C. Ji, B. Li, W. Liu, J. S. Smith, A. Majumdar, W. Luo, R. Ahuja, J. Shu, J. Wang, S. Sinogeikin, Y. Meng, V. B. Prakapenka, E. Greenberg, R. Xu, X. Huang, W. Yang, G. Shen, W. L. Mao, and H. K. Mao, *Nature* **573**, 558 (2019).
 - [3] Y. Akahama, N. Hirao, Y. Ohishi, and A. K. Singh, *J. Appl. Phys.* **116**, 223504 (2014).
 - [4] Y. Akahama, N. Okawa, T. Sugimoto, N. Hirao, and Y. Ohishi, *Jpn. J. App. Phys.* **57**, 025601 (2018).
 - [5] Y. Akahama, K. Takahashi, K. Kamiue, T. Sugimoto, N. Hirao, and Y. Ohishi, *J. Appl. Phys.* **125**, 075901 (2019).
 - [6] Y. Akahama, S. Kawaguchi, N. Hirao, and Y. Ohishi, *J. Appl. Phys.* **128**, 035901 (2020).
 - [7] Y. Akahama, S. Kawaguchi, N. Hirao, and Y. Ohishi, *J. Appl. Phys.* **129**, 135902 (2021).
 - [8] Y. Akahama, K. Kamiue, N. Okawa, S. Kawaguchi, N. Hirao, and Y. Ohishi, *J. Appl. Phys.* **129**, 025901 (2021).
 - [9] N. Hirao, Y. Akahama, and Y. Ohishi, *Matter Radiat. Extremes* **7**, 038403 (2022).
 - [10] P. Vinet, J. Ferrante, J. H. Rose, and J. R. Smith, *J. Geophys. Res.* **92**, 9319 (1987).
 - [11] F. Birch, *J. Geophys. Res.* **57**(2), 277 (1952).
 - [12] N. C. Holmes, J. A. Moriarty, G. R. Gathers, and W. J. Nellis, *J. Appl. Phys.* **66**, 2962 (1989).
 - [13] A. Dewaele, P. Loubeyre, and M. Mezouar, *Phys. Rev. B* **70**, 094112 (2004).
 - [14] D. E. Fratanduono, M. Millot, D. G. Braun, S. J. Ali, A. Fernandez-Pañella, C. T. Seagle, J.-P. Davis, J. L. Brown, Y. Akahama, R. G. Kraus, M. C. Marshall, R. F. Smit, E. F. O'Bannon III, J. M. McNaney, and J. H. Eggert, *Science* **372**, 1063 (2021):
 - [15] T. Funabiki, T. Sugimoto, N. Hirao, Y. Ohishi, and Y. Akahama, Special Issue of *Rev. High Pressure Sci. & Tech.* **24**, p. 203 (2014) (ISSN-0917-6373) in Japanese.
 - [16] Y. Akahama, H. Kawamura, and A. K. Singh, *J. Appl. Phys.* **95**, 4767 (2004): The data were revised using the latest Au EOS scale.
 - [17] K. Nakano, Y. Akahama, and H. Kawamura, *J. Phys.: Condens. Matter* **14**, 10569 (2002).
 - [18] W. B. Pearson: *Z. Kristallogr.* **126**, 362 (1968).
 - [19] P. Loubeyre, R. LeToullec, J. P. Pinceaux, H. K. Mao, J. Hu and R. J. Hemley, *Phys. Rev. Lett.* **71**, 2272 (1993).
 - [20] A. Dewaele, F. Datchi, P. Loubeyre, and M. Mezouar, *Phys. Rev. B* **77**, 094106 (2008)
 - [21] H. Fujihisa, Y. Akahama, H. Kawamura, Y. Ohishi, O. Shimomura, H. Yamawaki, M. Sakashita, Y. Gotoh, S. Takeya, and K. Honda, *Phys. Rev. Lett.* **97**, 085503 (2006).
 - [22] A. Dewaele, F. Datchi, P. Loubeyre, and M. Mezouar, *Phys. Rev. B* **77**, 094106 (2008).
 - [23] N. Nishimura, K. Kinoshita, Y. Akahama, H. Fujihisa, and H. Kawamura, *Proc. The 20th AIRAPT Int. Conf. on High Pressure Science and Technology, Karlsruhe*, edited by E. Dinjus, N. Dahmen, ISBN3-923704-49-6, T10-P054, p. 1-8, (2005).
 - [24] Y. Akahama, M. Nishimura, K. Kinoshita, H. Kawamura, and Y. Ohishi, *Phys. Rev. Lett.* **96**, 045505 (2006).
 - [25] S. J. Duclos, Y. K. Vohra, and A. L. Ruoff, *Phys. Rev. B* **41**, 12021 (1990).
 - [26] T. Sugimoto, Y. Akahama, H. Fujihisa, Y. Ozawa, H. Fukui, N. Hirao, and Y. Ohishi, *Phys. Rev. B* **86**, 024109 (2012).
 - [27] Y. Akahama, *Rev. High Pressure Sci. & Tech.* **16**, No.1, 137 (2006).
 - [28] A. Dewaele, F. Datchi, P. Loubeyre, and M. Mezouar, *Phys. Rev. B* **77**, 094106 (2008).
 - [29] Y. Akahama, H. Fujihisa, and H. Kawamura, *Phys. Rev. Lett.* **94**, 195503 (2005).
 - [30] S. Anzellini, D. Errandonea, L. Burakovsky, J. E. Proctor, R. Turnbull, and C. M. Beavers, *Sci. Rep.* **12**, 6727 (2022).
 - [31] H. Fujihisa and K. Takemura, *Phys. Rev. B* **52**, 13257 (1995).
 - [32] C. S. Yoo, H. Cynn, P. Söderlind, and V. Iota, *Phys. Rev. Lett.* **84**, 4132 (2000).
 - [33] A. Dewaele, P. Loubeyre, and M. Mezouar, *Phys. Rev. B* **70**, 094112 (2004).
 - [34] K. Takemura, K. Kobayashi, and M. Arai, *Phys. Rev. B* **58**, 2482 (1998).
 - [35] H. Fujihisa, *Rev. High Pressure Sci. & Tech.* **5**, 156 (1996) (in Japanese).
 - [36] A. D. Rosa, G. Garbarino, R. Briggs, V. Svitlyk, G. Morard, M. A. Bouhifd, J. Jacobs, T. Irifune, O. Mathon, and S. Pascarelli, *Phys. Rev. B* **97**, 094115 (2018).
 - [37] C. V. Storm, J. D. McHardy, S. E. Finnegan, E. J. Pace, M. G. Stevenson, M. J. Duff, S. G. MacLeod, and M. I. McMahon, *Phys. Rev. B* **103**, 224103 (2021).
 - [38] G. K. Samudrala, G. M. Tsoi, and Y. K Vohra, *J. Phys.: Condens. Matter* **24**, 362201 (2012).

- [39] S. Anzellini, F. Bottin, J. Bouchet, and A. Dewaele, Phys. Rev. B **102**, 184105 (2020).
- [40] K. Takemura and A. K. Singh, Phys. Rev. B **73**, 224119 (2006).
- [41] D. S. Mast, E. Kim, E. M. Siska, F. Poineau, K. R. Czerwinski, B. Lavina, and P. M. Forster, J. Phys. Chem. Solids **95**, 6 (2016).
- [42] S. Anzellini, D. Errandonea, C. Cazorla, S. MacLeod, V. Monteseguro, S. Boccato, E. Bandiello, D. D. Anichtchenko, C. Popescu, and C. M. Beavers, Sci. Reports **9**, 14459 (2019).
- [43] J. D. McHardy, C. V. Storm, M. J. Duff, C. M. Lonsdale, G. A. Woolman, M. I. McMahon, N. Giordano, and S. G. MacLeod, Phys. Rev. B **109**, 094113 (2024).
- [44] M. Forst, E. E. McBride, D. Smith, J. S. Smith, and S. H. Glenzer, J. Appl. Phys. **134**, 035901 (2023).
- [45] K. Takemura, Phys. Rev. B **56**, 5170 (1997).
- [46] A. Salamat, G. Garbarino, A. Dewaele, P. Bouvier, S. Petitgirard, C. J. Pickard, P. F. McMillan, and M. Mezouar, Phys. Rev. B, **84**, 140104(R) (2011).
- [47] R. Reichlin, A. K. McMahan, M. Ross, S. Martin, J. Hu, R. J. Hemley, H. K. Mao, and Y. Wu, Phys. Rev. B **49**, 3725 (1994).
- [48] H. Cynn, C. S. Yoo, B. Baer, V. Iota-Herbei, A. K. McMahan, M. Nicol, and S. Carlson, Phys. Rev. Lett. **86**, 4552 (2001).
- [49] W. Chen, D. V. Semenok, I. A. Troyan, A. G. Ivanova, X. Huang, A. R. Oganov, and T. Cui, Phys. Rev. B **102**, 134510 (2020).
- [50] L. Q. Huston, N. Velisavljevic, J. S. Smith, G. T. Gray, and B. T. Sturtevant, J. Phys.: Condens. Matter **34**, 055401 (2022).
- [51] S. Anzellini, A. Dewaele, F. Occelli, P. Loubeyre, and M. Mezouar, J. Appl. Phys. **115**, 043511 (2014).
- [52] C. S. Perreault, N. Velisavljevic, and Y. K. Vohra, Cogent Phys. **4**, 1376899 (2017).
- [53] C. V. Storm, G. A. Woolman, C. M. Lonsdale, J. D. McHardy, M. J. Duff, G. J. Ackland, and M. I. McMahon, Phys. Rev. B **109**, 024101 (2024).
- [54] Y. Akahama, H. Kawamura, and A. K. Singh, J. Appl. Phys. **92**, 5892 (2002).
- [55] K. Takemura, S. Nakano, Y. Ohishi, Y. Nakamoto, and H. Fujihisa, Mater. Res. Express **2**, 016502 (2015).
- [56] C. Cazorla, S. G. MacLeod, D. Errandonea, K. A. Munro, M. I. McMahon, C. Popescu, J. Phys.: Condens. Matter **28**, 445401 (2016).
- [57] H. K. Mao, Y. Wu, J. F. Shu, J. Z. Hu, R. J. Hemley, D. E. Cox, Solid State Commun. **74** 1027 (1990).
- [58] H. Olijnyk, J. Chem. Phys. **93**, 8968 (1990).
- [59] Y. Akahama, R. Miyamoto, S. Nakano, S. Kawaguchi, N. Hirao, and Y. Ohishi, J. Appl. Phys. **128**, 135901 (2020).

VII. FIGURE CAPTIONS

FIG. 1. (color online) $\log(V) - \log(P)$ plots for (a) Ni,[9] (b) Pt,[12–14] and (c) Bi.[15] Insets present results of the linear approximation in a pressure range between 200 and 300 GPa.

FIG. 2. (color online) Atomic number change of (a) V_{200} , V_{300} , (b) $V_{300}/V_{0\text{amb}}$ and (c) N -values for elements. Elements with P_{max} higher than ~ 200 GPa are shown in blue symbols. The recalculated results for Hf, Ta, and Pt are shown with red symbols.

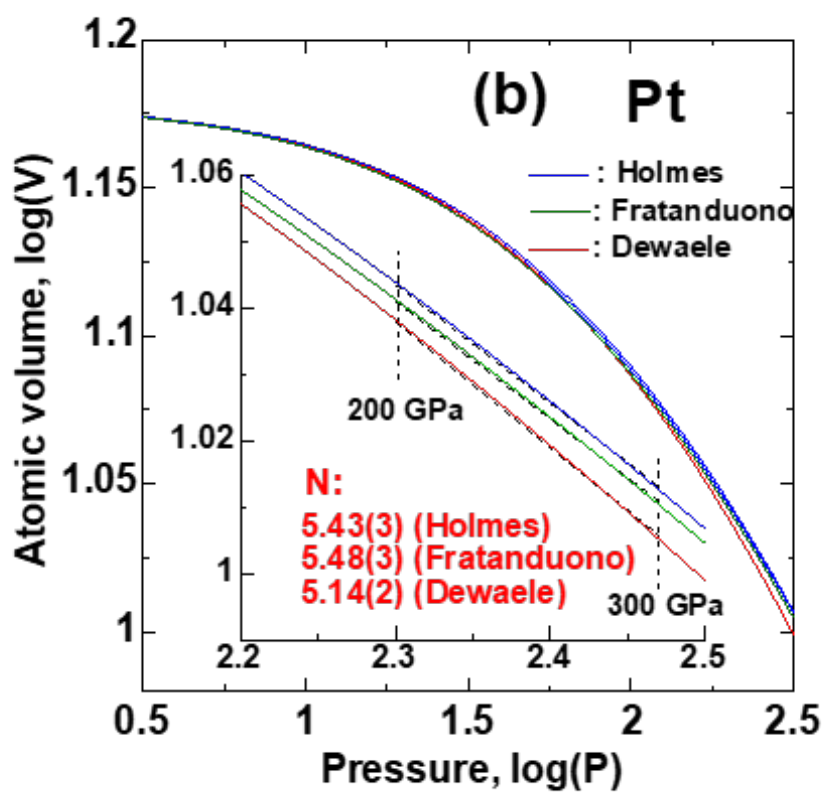
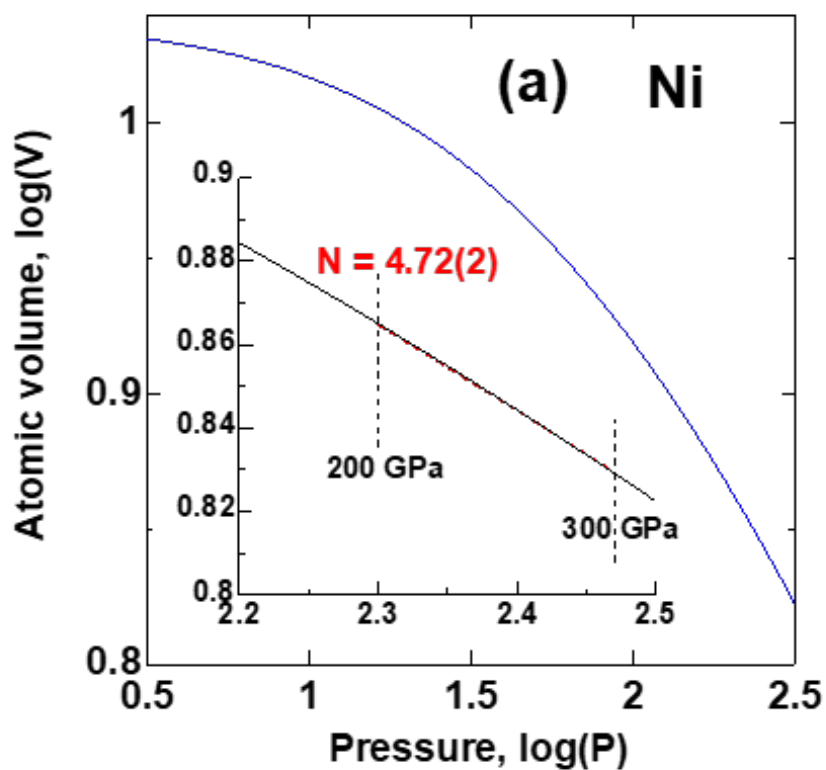
FIG. 3. (color online) P - V relation for molecular solids: H_2 , He, Ne, N_2 , [58] O_2 , Ar, Kr, and Xe. The values of volume for H, N, and O correspond to a single molecule: H_2 , N_2 , and O_2 . Arrows show the solidification pressure for each solid.

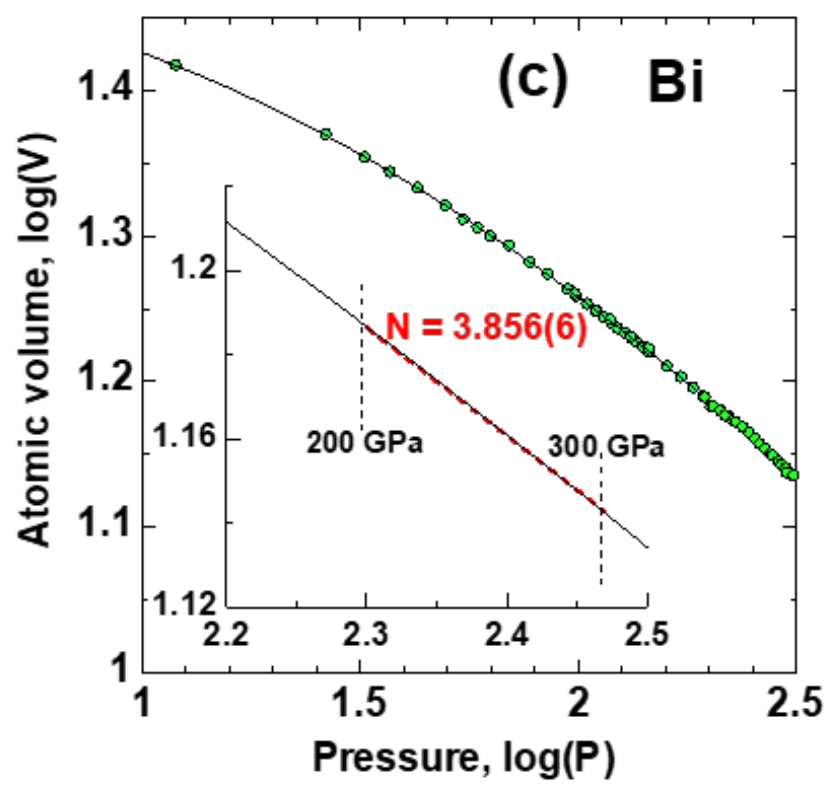
TABLE I. EOS data for elements and their analysis results: atomic No., element symbol, maximum pressure (P_{max} , GPa), atomic volume at ambient pressure (V_0 , \AA^3), bulk modulus (K_0 , GPa), pressure derivative of K_0 (K'_0), EOS formula, Vinet (V), Birch-Murnaghan (BM), and AP1 (polynomial, see Ref. 37), N value ($P \propto 1/V^N$), atomic volumes at 200 GPa and 300 GPa (V_{200} and V_{300} , \AA^3), atomic volume of ambient pressure phase under ambient condition ($V_{0\text{amb}}$, \AA^3), volume ratio ($V_{300}/V_{0\text{amb}}$), structure/phase, and reference No. The column of structure/phase shows the high-pressure structure or phase of the EOS based on the references (see the references for the structure notation and details). The values of volume for hydrogen, nitrogen, and oxygen correspond to a H_2 , N_2 , and O_2 molecule. The value of $V_{0\text{amb}}$ for rare gases, hydrogen, nitrogen, and oxygen are correspond to V_0 in this table.

Fig. 1. The $\log(V) - \log(P)$ plots for (a) Ni[9], (b) Pt[12–14] and (c) Bi[15]. Insets present results of the linear approximation in a pressure range between 200 and 300 GPa.

Fig. 2. Atomic number change of (a) V_{200} , V_{300} , (b) $V_{300}/V_{0\text{amb}}$ and (c) N -values for metallic elements. Elements with P_{max} higher than about 200 GPa are shown in blue. The recalculated results for Hf, Ta and Pt are shown with red symbols.

Fig. 3. P - V relation for molecular solids: H_2 , He, Ne, N_2 [57], O_2 , Ar, Kr, and Xe. The values of volume for H, N, and O correspond to one molecule: H_2 and N_2 , and O_2 . Arrows show the solidification pressure for each solid.





Atomic No.	Atom	P_{\max}	V_0	K_0	K'_0	EOS	N, V^{-N}	V_{200}	V_{300}	$V_{0\text{amb}}$	$V_{300}/V_{0\text{amb}}$	Structure /phase	Ref.
1	H	190	42.246	0.110(6)	7.36(7)	V	2.273(3)	3.6	3.01	42.25	0.071	hcp	2
2	He	58	22.79	0.225	7.35	V	2.461(3)	3.38	2.20	22.79	0.097	fcc-hcp	19
4	Be	171	8.066	97.2(2.5)	3.61(7)	BM	3.05(1)	4.19	3.66	8.07	0.454	hcp	17
4	Be	-	8.066	96.59(5)	3.758(3)	V	2.99(1)	4.18	3.64	8.07	0.451	-	revised
6	C	80	5.669	444.5	4.18	V	5.29(3)	4.36	4.03	5.669	0.711	diamond	20
8	O	96	36.73	1.79(2)	8.06(3)	V	3.474(4)	9.80	8.72	36.73	0.237	ϵ -O ₂	21
10	Ne	208	22.234	1.07(2)	8.40(3)	V	3.465(4)	5.41	4.81	22.23	0.216	fcc	22
12	Mg	158	19.95	68.7	3.47	V	2.55(1)	8.89	7.59	23.22	0.327	bcc	23
13	Al	333	16.597	72.7	4.83	V	3.44(1)	8.67	7.71	16.6	0.464	fcc-hcp	24
14	Si	248	14.329	82	4.22	BM	3.654(8)	7.62	6.82	20.02	0.341	hcp	25
15	P	340	10.661	254(16)	4.34(44)	V	2.71(1)	8.01	7.14	37.8	0.378	sh	26
16	S	255	9.25	495(12)	3.91(46)	V	2.66(2)	8.33	7.44	25.73	0.289	β -Po	27
18	Ar	248	37.45	2.65	7.56(2)	v	3.358(4)	10.37	9.20	37.45	0.246	fcc	28
21	Sc	300	15	98.5(1.0)	5.28(4)	V	3.91(1)	8.71	7.95	24.79	0.32	hexagonal	29
22	Ti	290	15.97(4)	125(2)	3.46(6)	BM	3.20(2)	8.9	7.84	17.74	0.442	delta-bcc	6
23	V	290	13.87(2)	156(6)	4.3(1.6)	V	4.12(2)	8.67	7.86	13.87	0.567	bcc-rhombo.	7
24	Cr	133	12.04(1)	182(1)	5.10(4)	V	4.48(2)	8	7.31	12.04	0.607	hcp	30
25	Mn	190	12.66	158	4.6	BM	4.41(1)	8.1	7.39	14.14	0.522	α -Mn	31
26	Fe	355	11.22(3)	159.3(1.0)	5.86(4)	V	5.14(2)	7.47	6.87	11.75	0.585	hcp	9
27	Co	210	10.34	224	5.8	V	5.67(2)	7.37	6.85	11.01	0.623	fcc	32
28	Ni	370	10.9376(4)	173.5(1.4)	5.55(5)	V	4.72(2)	7.23	6.71	10.94	0.613	fcc	9
29	Cu	144	11.81	132.4(1.4)	5.32(6)	V	4.26(2)	7.4	6.77	11.81	0.573	fcc	33
30	Zn	257	15.12(6)	63(2)	5.4(3)	BM	4.237(6)	8.22	7.47	15.12	0.494	hcp	8
31	Ga	100	18.23(19)	55(5)	4.7(5)	BM	3.806(5)	9.13	8.21	19.6	0.419	fcc	34
32	Ge	258	14.10(2)	313(2)	3.27(4)	BM	3.85(2)	9.81	8.83	22.64	0.39	hcp	8
33	As	247	16.25(3)	182(1)	3.67(3)	BM	3.668(8)	10.15	9.09	21.51	0.423	bcc	8
34	Se	320	15.52(9)	290(6)	3.20(7)	BM	3.61(2)	10.55	9.43	27.27	0.346	bcc	8
35	Br	80	32.73	14.1	4.6	BM	3.350(3)	11.06	9.83	42.54	0.231	bet	35
36	Kr	140	37.47	3.03	7.24	V	3.243(4)	10.28	9.07	37.47	0.242	fcc-hcp	36
37	Rb	264	92.9(4)	0.15(3)	7.66(15)	AP1	3.166(2)	12.28	10.81	92.90	0.116	tI4-oC16	37
39	Y	177	22.45	108	3.4	BM	2.72(1)	11.65	10.03	32.9	0.305	$C2/m$	38
40	Zr	142	22.6	93(1)	3.20(9)	V	2.59(1)	10.89	9.31	23.29	0.4	bcc	39
41	Nb	134	18.008	151(3)	4(1)	BM	3.18(1)	10.73	9.46	18.01	0.525	bcc	40
42	Mo	410	15.58(1)	262(4)	4.55(16)	V	4.60(2)	10.95	10.03	15.58	0.644	bcc	3
43	Tc	67	14.31	309(7)	4.7(4)	V	4.96(2)	10.425	9.606	14.31	0.671	hcp	41
44	Ru	151	13.565(2)	319.1(9)	4.40(2)	V	4.78(1)	9.858	9.057	13.565	0.668	hcp	42
45	Rh	191	13.764(2)	257(2)	5.44(8)	V	5.18(2)	9.9	9.15	13.76	0.654	fcc	43
46	Pd	182	14.669(18)	189.3(30)	5.473(63)	V	4.78(2)	9.98	9.15	14.67	0.624	fcc	44
47	Ag	165	17.051(8)	99.0(4)	6.19(3)	V	4.56(2)	10.46	9.57	17.05	0.561	fcc	15
48	Cd	174	21.578	42(1)	6.5(2)	BM	4.42(1)	11.31	10.32	21.58	0.478	hcp	45
49	In	250	26.18(1)	32.7(10)	6.28(25)	BM	4.234(6)	12.83	11.66	25.97	0.449	dis. fcc	5
50	Sn	194	13.96(6)	652(20)	4	BM	4.026(4)	13.15	11.9	27.04	0.44	hcp	46
51	Sb	253	27.95(8)	36.5(5)	6.28(5)	V	3.853(8)	13.68	12.31	34.87	0.353	bcc	5
52	Te	330	23.95(14)	121(3)	4.54(8)	V	3.660(9)	14.05	12.57	34.01	0.37	fcc	4
53	I	276	31.25(7)	30.38(13)	6.13(1)	V	3.660(9)	14.41	12.91	40.9	0.316	fcc	47
54	Xe	200	63.073	4.3(3)	4.9(1)	BM	3.309(1)	15.77	13.95		0.221	hcp	48
57	La	140	37.5	14.5(1)	5	BM	3.549(3)	13.53	12.08	37.19	0.325	dis. fcc	49
72	Hf	120	21.5(2)	109.8(5.2)	3.10(5)	BM	2.31(1)	10.52	7.81	22.3	0.35	bcc	50
72	Hf	-	15.32	279.28(8)	2.079(5)	V	2.48(1)	10.82	9.18	22.3	0.412	-	revised
73	Ta	90	18.035	197.0(3.5)	3.39(15)	V	3.38(2)	11.23	9.96	18.04	0.552	bcc	13
73	Ta	-	18.035	-	-	V	3.63(2)	11.4	10.17	18.04	0.564	-	revised
74	W	155	15.862	295.2(3.9)	4.32(11)	V	4.60(2)	11.32	10.79	15.86	0.598	bcc	13
75	Re	144	14.733	352.6	4.56	V	5.08(2)	10.96	10.12	14.73	0.687	hcp	51
76	Os	207	14.01	444	3.99	BM	5.31(2)	10.75	9.96	14.01	0.711	hcp	52
77	Ir	159	14.153(3)	351(3)	5.29(9)	V	5.72(1)	10.75	10.04	14.15	0.71	fcc	53
78	Pt	800	15.102	259.7(2)	5.839(3)	V	5.48(3)	10.99	10.21	15.1	0.676	fcc	14
78	Pt	660	15.1	278	5.61	V	5.43(2)	11.057	10.262	15.102	0.68	fcc	12
78	Pt	100	15.095	273.6(2.0)	5.23(8)	V	5.14(2)	10.91	10.09	15.1	0.668	fcc	13
79	Au	222	16.929	170.9(2)	5.880(5)	V	4.94(2)	11.44	10.53	16.93	0.622	fcc	14,54
80	Hg	197	16.84(4)	251(9)	4.5(2)	V	4.02(1)	12.18	11.01	24.5	0.449	hcp	55
81	Tl	125	28.2(2)	48(4)	4	BM	3.175(4)	12.52	11.02	28.8	0.383	fcc	56
82	Pb	238	29.8	39.9	6.13	V	3.82(1)	14.75	13.27	30.33	0.438	bcc	57
83	Bi	332	31.44(6)	38.20(29)	6.229(32)	V	3.856(6)	15.51	13.96	34.44	0.405	bcc	15

